



ORIGINAL RESEARCH PAPER

The Protective Effect of Thiamine on the Histo-stereological Structural Changes of the Testicles and Oxidative State Induced by Copper Oxide Nanoparticles in Rat

Jahangir Kaboutari*, Rahmat Allah Fatahian Dehkordi

Department of Basic Sciences, Faculty of Veterinary Medicine, Shahrekord University, Shahrekord, Iran.

Article info

Article history:

Received 2026-02-01

Received in revised form
2026-02-21

Accepted 2026-02-22

Keywords:

Germinal Layers

Histostereology

CuO NPs

Thiamine

Abstract

Nanoparticles represent an innovative and highly promising technology in the fields of medicine and diagnostics, offering unique capabilities for targeted drug delivery and advanced diagnosis. This study aimed to investigate the protective effects of thiamine against the histo-stereological and biochemical alterations induced by copper oxide nanoparticles (CuO NPs) in the testes. A total of 72 adult male, healthy Wistar rats were divided into four groups: control, thiamine (30 mg/kg), CuO NP (25 mg/kg), and a combination of CuO NPs and thiamine (30 mg/kg + 25 mg/kg). All substances were administered via intraperitoneal injection, once daily. After 14 days of treatment, the tissue and blood samples were collected for histo-stereological evaluation and total antioxidant capacity (TAC), malondialdehyde (MDA), superoxide dismutase (SOD) catalase (CAT) antioxidant enzymes, body weight and testicular weight assessment. Control and thiamine groups maintained normal seminiferous tubule structure, regular spermatogenesis, and high antioxidant levels. CuO NPs administration induced severe histopathological damages, including significant reduction in seminiferous tubule diameter, disruption of the germinal epithelium, a significant decrease in the number of spermatocytes and spermatids, a significant decrease in body and testicular weight, and diminished antioxidant enzyme activity ($P < 0.05$). Thiamine exerts protective effects in testicular tissue through its antioxidant, anti-inflammatory and anti-apoptotic properties, and may serve as an effective adjunct therapeutic agent to counteract the reproductive toxicity and adverse effects induced by CuO NPs.

1. Introduction

CuO NPs constitute a significant class of inorganic nanomaterials distinguished by a suite of unique physicochemical attributes including specific optical, thermal, and magnetic properties, in addition to enhanced electrical conductivity, high catalytic activity, and a substantial surface-to-volume ratio. Notably,

CuO NPs demonstrate a potent bactericidal effect coupled with considerable antiviral and antifungal efficacy, underscoring their utility in biomedical and therapeutic domains. Current research is extensively exploring their role in wound healing protocols, advanced drug delivery systems, and as cytotoxic agents in oncology treatments (1–6). Despite their increasing utility, the pervasive application of CuO NPs necessitates a crit-

*Corresponding author: J. Kaboutari (Associate Professor)

E-mail address: kaboutari-j@sku.ac.ir

<http://dx.doi.org/10.22084/AVR.2026.32275.1029>

ical evaluation of potential toxicological profile, particularly concerning reproductive health. Exposure to CuO NPs has been shown to induce detrimental effects on both the male and female reproductive systems. The mechanism of action frequently involves the induction of oxidative stress, inflammatory responses, generalized cellular damage, and apoptosis. Specifically, the generation of reactive oxygen species (ROSs), often exceeding the endogenous antioxidant capacity of the organism, precipitates substantial peroxidation of lipids and degradation of proteins. This resultant oxidative damage critically impairs spermatogenesis, leading to a measurable reduction in sperm count, diminished motility, and compromised overall semen quality. Furthermore, elevated ROSs levels can induce DNA fragmentation, which fundamentally jeopardizes male fertility. In the testes, inflammation mediated by CuO NPs can severely restrict spermatogenesis, induce structural damage to the seminiferous tubules, and alter the integrity of the blood-testis barrier function, culminating in infertility (3, 7, 8).

Beyond cellular damage, CuO NPs possess the capacity to interfere with the endocrine system by disrupting androgenic hormone regulation. Such disruption can manifest as reduced libido, decreased spermatogenic output, and potentially contribute to erectile dysfunction. The induction of apoptosis within spermatogenic cells further exacerbates the decline in germ cell populations (3, 7, 8). For maternal exposures, the potential for placental barrier penetration by CuO NPs raises significant concerns, as this can lead to fetal growth restriction, congenital anomalies, and developmental deficits in the offspring, with particular vulnerability noted in the development of the reproductive organs (3, 7, 8).

Thiamine (Vitamin B1) is an essential water-soluble vitamin, crucial for the development and physiological function of various cell types. Its metabolic significance is profound, serving as a coenzyme in key pathways, including energy metabolism, lipid synthesis, and nucleotide formation. It is also critically involved in neural cell development and enhances endothelial cell function (9). Crucially, thiamine exhibits inherent antioxidant properties. It acts as an essential cofactor under physiological stress, providing demonstrated protection against lead-induced lipid peroxidation in hepatic and renal tissues. Functioning as an effective scavenger of superoxide and hydroxyl anion free radicals, thiamine significantly augments the cellular response mechanisms to oxidative stress. Preclinical models have shown that thiamine effectively mitigates nanoparticle-induced nephrotoxicity (9).

Acknowledging that CuO NPs induce reproductive toxicity via oxidative stress and inflammatory cascades, and given the established antioxidant properties of thiamine, this investigation will meticulously examine the resulting histo-stereological and oxidative dam-

age in the testicles, while simultaneously assessing the potential ameliorative effects of thiamine.

2. Materials and Methods

CuO NPs, supplied by Sigma-Aldrich (USA), were used. The manufacturer specified a 99% purity, particle size of approximately 50 nm, a density of 6.4 g/cm³, a specific surface area of 20 m²/g, and appear as black spherical crystalline structures.

3. Animal Experimental Design and Protocols

A total of 72 healthy adult male Wistar rats, weighing between 200–250 grams, were utilized in accordance with established institutional and international animal care and use guidelines. They were maintained in standard polycarbonate cages under controlled environmental conditions, specifically a 12-hour light/12-hour dark cycle, a stable ambient temperature of 22±2°C, and a relative humidity of 55%–60% (23).

Prior to the commencement of the experiments, animals underwent a one-week period of acclimatization. Following this period, they were randomly allocated into four experimental groups, with each group comprising 18 animals (three replicates with n=6 each). All substances were prepared using sterile normal saline, and administered via intraperitoneal injection for a duration of two consecutive weeks, with injections performed once daily. The volume of administration for all injections was consistently 1 mL (23).

Group 1 served as the control and received only normal saline, whereas Groups 2, 3, and 4 were treated with 30 mg/kg of thiamine, 25 mg/kg of CuO NPs, and a combination of 30 mg/kg of thiamine and 25 mg/kg of CuO NPs, respectively. The doses of 25 mg/kg for CuO NPs and 30 mg/kg for thiamine were chosen based on previous experimental studies. CuO NPs at 25–35 mg/kg have been shown to induce testicular oxidative damage in rodents (Naz et al., 2023). Thiamine at comparable intraperitoneal doses has demonstrated antioxidant and protective effects in rodent models of oxidative stress (Amiri et al., 2018). The suspension of CuO NPs was vigorously sonicated for 30 minutes immediately prior to each daily administration to ensure a homogeneous dispersion. The pH of all final solutions and suspensions was carefully adjusted to 7.0–7.4.

At the end of the 14-day treatment period, rats were weighed using a digital analytical balance (accurate to 0.01 g) prior to euthanasia. Both testes were carefully excised from the scrotum, gently cleaned of surrounding tissues, and weighed individually using the same balance. All weights were recorded as fresh, unfixed tissue immediately after dissection to ensure accuracy. Upon completion of the 14-day experimental period,

blood samples for subsequent biochemical analysis were collected from all animals via cardiac puncture (24). Following blood collection, the rats were immediately euthanized through the intraperitoneal administration of 150 mg/kg of sodium pentobarbital (Sigma-Aldrich, USA), and the testes were then carefully excised from the scrotal sac for further tissue analyses (23).

4. Stereology

After excision of the testes and careful removal of surrounding tissues, the primary volume (V_{primary}) of each testis was determined using the immersion method (25). To achieve isotropic uniform random (IUR) sampling, the Orientator method was applied. Ten serial sections with a thickness of 5 μm were randomly selected per testis (25, 9).

For stereological analysis, ten slides per animal were examined, and within each slide, ten non-overlapping fields of view (FOV) were captured at 400 \times magnification, resulting in a total of 100 FOV per animal (25, 9). Volume densities (V_v) of seminiferous tubules, interstitial tissue, primary spermatocytes, and spermatids were quantified using the point-counting method, calculated as the ratio of points hitting the structure of interest to the total number of test points (25).

Tissue processing was performed using an automated processor (Leica TP 1020, Germany), and sections were stained with Hematoxylin and Eosin (H&E) for standard histological evaluation. Ten randomly selected slides per animal were examined, and within each slide, ten distinct fields of view were captured, resulting in 100 FOV per animal. Quantitative measurements included seminiferous tubule diameter, germinal epithelium height, and volume densities of seminiferous tubules, interstitial tissue, primary spermatocytes, and spermatids. All measurements were independently performed by two blinded observers, and any discrepancies were resolved through joint reevaluation to ensure accuracy and reproducibility (25, 9).

After excision of the testes and careful removal of surrounding tissues, the primary volume (V_{primary}) of each testis was determined using the immersion method (25). To achieve isotropic uniform random (IUR) sampling, the Orientator method was applied. Ten serial sections with a thickness of 5 μm were randomly selected per testis (25,9).

5. The Number of Cells and the Diameter of the Tubes

For the quantification of spermatogenic cells and measurement of seminiferous tubule diameter, the same sections used for stereological analysis were examined. Ten randomly selected slides per animal were analyzed, and within each slide, ten non-overlapping fields of

view (FOV) were systematically examined, resulting in 100 FOV per animal (25, 9).

Primary spermatocytes and spermatids were identified and counted based on established morphological criteria and their relative positions within the seminiferous tubules (9). Seminiferous tubule diameter was measured using a calibrated ocular micrometer at 400 \times magnification, consistent with the magnification used for stereological assessment (25, 9).

All stereological parameters, including volume densities of seminiferous tubules, interstitial tissue, primary spermatocytes, and spermatids, were recorded for each tubule. This approach ensured that measurements of tubule diameter and cell counts were directly correlated with stereological observations.

All measurements and cell counts were independently performed by two blinded observers to prevent bias. Any discrepancies were resolved through joint reevaluation to ensure accuracy and reproducibility (25, 9). The resulting mean values provided reliable and reproducible data for the assessment of testicular structure, spermatogenic integrity, and the potential protective effects of thiamine against CuO NP-induced damage.

6. Antioxidant Enzyme Assessment

A colorimetric technique utilizing commercial kits (Navand Salamat, Urmia, Iran) was employed to quantify Catalase activity. The reaction mixture consisted of 30 mM phosphate buffer (pH 7.0), 2.9 mL of hydrogen peroxide, and 0.1 mL of serum. The consumption of hydrogen peroxide was monitored, and the absorbance was measured at a wavelength of 550 nm (UNICO, SQ 2800, China). Catalase activity was expressed in units per liter (U/L).

SOD Enzyme activity was measured using commercial kits (Navand Salamat, Urmia, Iran), based on the inhibition of pyrogallol autoxidation and expressed as units per liter (U/L).

MDA is derived from the decomposition of polyunsaturated fatty acids. A colorimetric assay was employed, based on the interaction between MDA and thiobarbituric acid (TBA) to form a pink-colored complex that can be measured spectrophotometrically at 532 nm. The TBA reagent was prepared by mixing equal volumes of a 15% (v/v) trichloroacetic acid (TCA) solution, a 0.375% (v/v) thiobarbituric acid solution, and 0.25 N hydrochloric acid. A 2 mL aliquot of the reagent was added to 1 mL of serum, and the mixture was incubated in a boiling water bath for 50 minutes. After incubation, the sample was cooled for 10 minutes, then centrifuged at 1000 g for 10 minutes at 4°C. The absorbance of the supernatant was measured at 532 nm (UNICO, SQ 2800, China). The concentration of MDA was determined using the molar

absorption coefficient in phosphate buffer (6).

The ferric reducing antioxidant power (FRAP) method was used to quantify Total Antioxidant Capacity using spectrophotometry at a wavelength of 593 nm (UNICO, SQ 2800, China). This method was based on the reduction of ferric ions to ferrous ions by the reducing power of antioxidant compounds present in plasma. The results are expressed as micromoles per liter (mol/L).

7. Statistical Analysis

All data are presented as mean \pm standard error of the mean (SEM). Prior to statistical comparisons, datasets were tested for normality using the Shapiro–Wilk test and the homogeneity of variances among groups was assessed using Levene’s test. Once the assumptions of normality and equal variances were confirmed, one-way analysis of variance (ANOVA) was performed, followed by Tukey’s post-hoc test for multiple comparisons. Differences were considered statistically significant at $P < 0.05$.

8. Results

8.1. Histomorphometry

Histological examination of the control group revealed a typical, compact architecture within the testicular tissue. The seminiferous tubules were maintained a dense structure and exhibited a demonstrably normal spermatogenesis process. Specifically, the reproductive epithelium lining the seminiferous tubules displayed a regular, stratified arrangement. Proper cell-to-cell junctions were clearly discernible between the different germinal cell populations. The cellular layers were organized in the expected sequential order, consisting of basal spermatogonia, followed by spermatocytes, spermatids, and finally, spermatozoa (mature sperm cells). The intact cellular connectivity and the sequential stratification of the germ cells within these tubules serve as evidence of the uninterrupted differentiation of the primary germ line into mature gametes (Figs. 1(A) and 2(A1)).

Histological analysis of the group treated with thiamine demonstrated testicular morphology highly comparable to that of the control group. The seminiferous tubules maintained normal architecture and the germinal cells within were arranged in a regular, orderly fashion. The unimpaired spermatogenic process was observed, exhibiting a clear and sequential organization of the germ cell line. The tubules were well-defined, containing a substantial population of germ cells, which included the full sequence of development from spermatogonia through to spermatozoa. Additionally, the interstitial tissue presented a normal configuration, and the intercellular spacing within the

tubules appeared normal. Overall, the thiamine group showed no significant deviation from the control, confirming preserved spermatogenesis and structural integrity (Figs. 1(B) and 2(A2)).

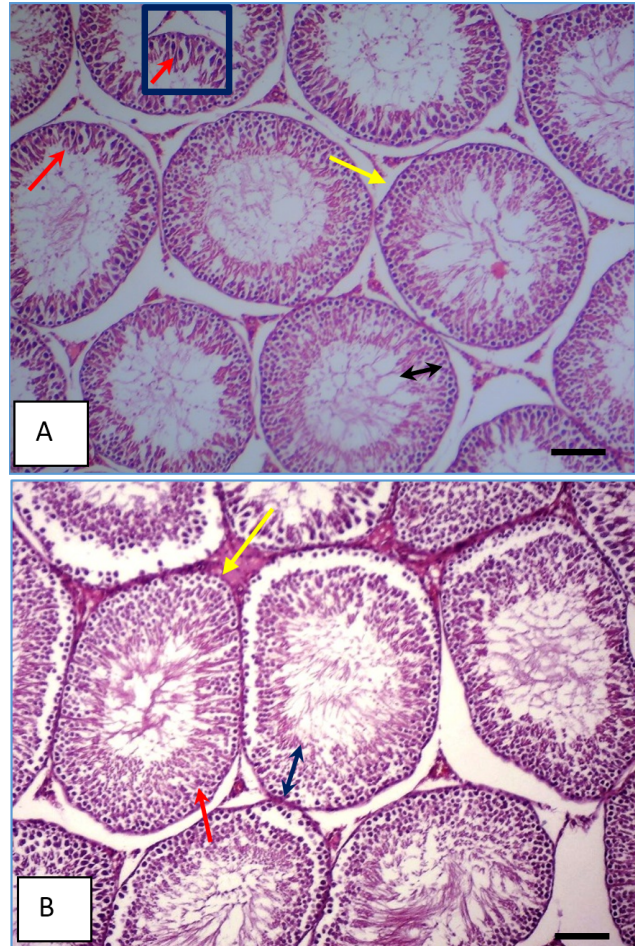


Fig. 1. Light microscope photomicrograph of the testicular tissue from adult mice in the control A) and thiamine B) groups; a normal shape of the seminiferous tubules (yellow arrow) with a normal germ wall (black arrow) along with the germ cell line "primary spermatocytes" (red arrow with magnification) is observed; (magnification 200 \times , H&E staining).

CuO NPs-treated group revealed severe structural and cellular anomalies within the testicular tissue, indicating significant spermatogenic disruption. The seminiferous tubules exhibited marked irregularities and disorganization. A notable finding was the premature sloughing of spermatogonia, spermatocytes, and spermatids into the tubular lumen, frequently accompanied by a marked reduction in the density of these germ cell populations. Crucially, the basal integrity of the tubules was compromised, evidenced by the separation and degeneration of spermatogonia from the basement membrane. These pathological changes resulted in the irregularity and disorganization of the reproductive epithelium, leading to a noticeable decrease in epithelial

height and a corresponding enlargement of the seminiferous tubule lumen. Furthermore, the interstitial tissue surrounding the tubules was distinctly edematous. Signs of acute inflammation were also evident, including vascular congestion and widespread cellular damage, characterized by eosinophilic cytoplasm and pyknotic nuclei (Figs. 2(B1) and B2).

In the CuO NPs + Thiamine group, the majority of the destructive changes and irregularities induced by CuO NPs were reversed and ameliorated. As a result, the reproductive epithelium of the seminiferous tubules exhibited an almost normal structure (Figs. 2(C1) and C2).

8.2. Stereology

The diameter of the seminiferous tubules in the CuO NPs group was significantly reduced compared to the

control group. Conversely, the CuO NPs + Thiamine group showed a significant increase in tubule diameter when compared specifically to the CuO NPs group ($P < 0.05$). Regarding stereological parameters (Table 1), the CuO NPs group exhibited a significant decrease in the mean volume density (V_v) of the seminiferous tubules ($60.25\% \pm 5.36$) compared to the control group ($86.45\% \pm 6.39$) ($P < 0.05$). Correspondingly, the V_v of the interstitial tissue was significantly increased in the CuO NPs group ($36.17\% \pm 1.67$) relative to the control ($9.43\% \pm 3.27$) ($P < 0.05$), reflecting severe tissue damage and edema. Furthermore, the V_v of the germinal cells, primary spermatocytes ($17.34\% \pm 2.27$) and spermatids ($21.2\% \pm 1.15$), were both significantly decreased in the CuO NPs group compared to the control ($32.4\% \pm 3.01$ and $45.6\% \pm 4.25$) respectively ($P < 0.05$).

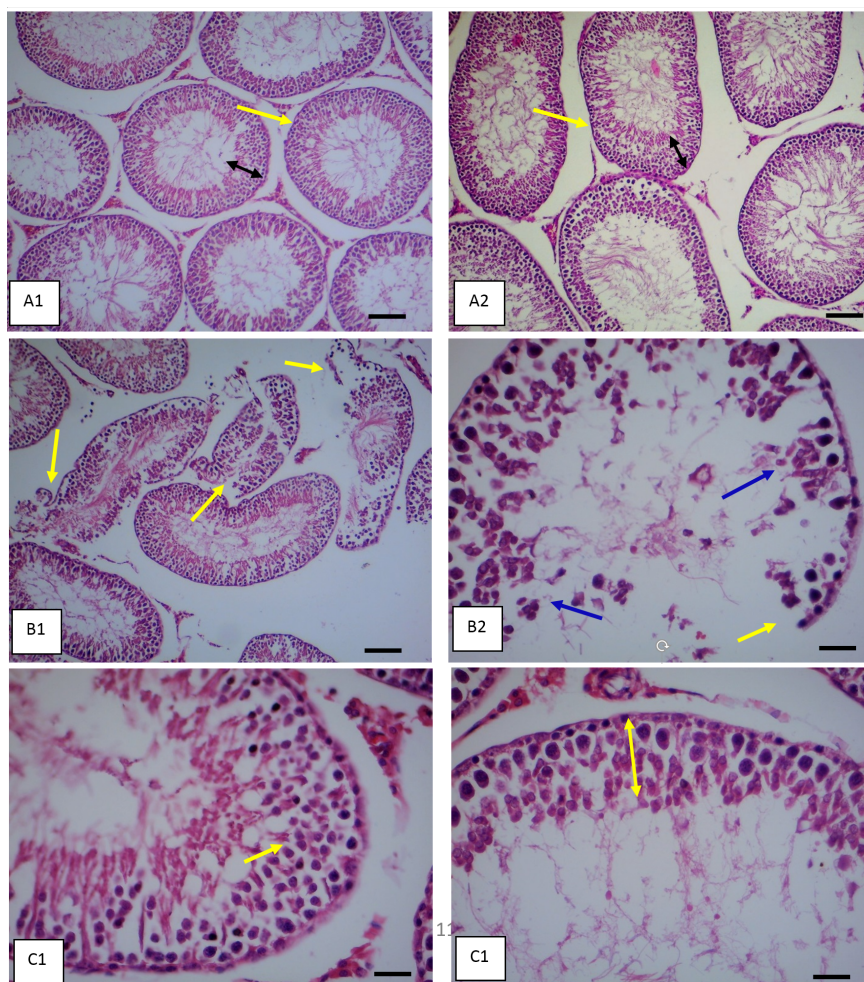


Fig. 2. Light microscope photomicrograph of testicular tissue from adult mice in the control (A1, A2), CuO NPs (B1, B2) and CuONPs+ Thiamine (C1, C2) groups. In the control group (A1, A2), the complete histological structure of the seminiferous tubules (yellow arrow) with a normal germinal wall (black arrow) has been seen. In the CuO NPS group (B1, B2), the germinal epithelium of the seminiferous tubules lost its integrity (yellow arrow) and the spermatogenic cells of the germinal wall had disintegrated (blue arrow). In the CuO NPs+ Thiamine (C1, C2) group, the germinal epithelium had largely maintained its normal structure and was improved (yellow arrow; magnification 200 \times , H&E staining).

Table 1

Mean volume densities (%) of seminiferous tubules, interstitial tissue, and germinal cells in all experimental groups.

Group	Group			
	Control	Thiamine	CuO NPs	CuO NPs+ Thiamine
Parameters				
Volume density (%)				
Seminiferous tubules	86.45±6.39 ^a	82.48±6.34 ^a	60.25±5.36 ^b	79.32 ± 6.54 ^a
Interstitial tissue	9.43±3.27 ^a	10.36±2.89 ^a	36.17±1.67 ^b	9.87±2.71 ^a
Primary spermatocyte	32.4±3.01 ^a	28.14±3.11 ^a	17.34±2.27 ^b	22.5±1.19 ^a
Spermatids	45.6±4.25 ^a	40.2±3.96 ^a	21.2±1.15 ^b	31.3±2.75 ^a

a/b letters: Different letters indicate statistically significant differences between groups (P<0.05)

Table 2

Mean number of spermatocytes, spermatids, and seminiferous tubule diameter (m) in all experimental groups.

	Group			
	Control	Thiamine	CuO NPs	CuO NPs+ Thiamine
Diameter (μm)				
Tubules	242±26 ^a	240±25 ^a	179±20 ^b	237±18 ^a
Number				
Spermatocyte	23.4±2.04 ^a	22.1±1.36 ^a	11.6±1.02 ^b	18.7±2.15 ^a
Spermatid	47.2±3.58 ^a	53.9±4.68	17.3±3.81 ^b	38.4±4.60 ^a

a/b letters: Different letters indicate statistically significant differences between groups (P<0.05)

Table 3

Mean body weight and testes (gr) and diameter seminiferous tubules (μm) in all groups

	Group			
	Control	Thiamine	CuO NPs	CuO NPs+ Thiamine
Parameters				
Weight (gr)				
Testis	1.78±0.08 ^a	1.71±0.08 ^a	1.28±0.07 ^b	1.62±0.09 ^a
Body	210.4±4.3 ^a	224.4±4.4 ^a	171.3±3.85 ^b	207±4.5 ^a

a/b letters: Different letters indicate statistically significant differences between groups (P<0.05)

In contrast, treatment with thiamine significantly mitigated these adverse effects. The CuO NPs + Thiamine group demonstrated a significant increase and structural improvement in the Vv of the seminiferous tubules (79.32%±6.54), primary spermatocytes (22.5%±1.19), and spermatids (31.3%±2.75) compared to the CuO NPs group (P< 0.05). This recovery was concurrently reflected by the significant decrease in the Vv of the interstitial tissue (9.87% ±2.71) in the combined treatment group compared to the CuO NPs group (P<0.05) (Table 2).

Different letters (a&b) indicate significant differences between different treatment groups (P< 0.05); data are presented as Mean ± SEM.

Additionally, there was a significant decrease in the number of spermatocytes and spermatids in the CuO NPs group compared to the control (P<0.05). In contrast, a significant increase in the number of spermatocytes and spermatids was noted in the CuO NPs + Thiamine group compared to the CuO NPs group

(P<0.05) (Table 2).

8.3. Body and Testicle Weights

At the conclusion of the experiments, analysis revealed no significant difference in the mean body weight or mean testicular weight among the Control, Thiamine-alone, and the CuO NPs+Thiamine co-administration groups (p>0.05). Conversely, the CuO NPs group exhibited a significant decrease in both mean body weight and mean testicular weight when compared to all other experimental groups (p<0.05).

8.4. Antioxidants Assessment

The Control and Thiamine-alone groups did not differ statistically in the measured CAT enzyme activity (0.05). Conversely, both the CuO NPs and the CuO NPs + Thiamine groups exhibited a significant decrease in enzyme activity when compared to both the Control and Thiamine groups (0.05) (Table 4).

Table 4

CAT changes (nm/ml) in the experimental groups.

	Groups days			
	Control	Thiamine	CuO NPs	CuO NPs+ Thiamine
14	176.7±11.89 ^a	178.2±12.18 ^a	145.2±8.36 ^b	150.4±10.01 ^b
<i>P value</i>	<i>p>0.05</i>	<i>p>0.05</i>	<i>P<0.05</i>	<i>p>0.05</i>

a/b letters: Different letters indicate statistically significant differences between groups (P<0.05)

Table 5

SOD changes (nm/ml) in the experimental groups.

	Groups days			
	Control	Thiamine	CuO NPs	CuO NPs+ Thiamine
14	22/74±3/57 ^a	22/74±3/57 ^a	41/52±5/37 ^b	29/71±4/28 ^b
<i>P value</i>	<i>p>0.05</i>	<i>p>0.05</i>	<i>P<0.05</i>	<i>p>0.05</i>

a/b letters: Different letters indicate statistically significant differences between groups (P<0.05)

Table 6

TAC changes (nm/ml) in the experimental groups.

	Groups days			
	Control	Thiamine	CuO NPs	CuO NPs+ Thiamine
14	0.12±0.02 ^a	0.10±0.02 ^a	0.08±0.01 ^b	0.11±0.02 ^a
<i>P value</i>	<i>p>0.05</i>	<i>p>0.05</i>	<i>P<0.05</i>	<i>p>0.05</i>

a/b letters: Different letters indicate statistically significant differences between groups (P<0.05)

Table 7

MDA changes (nm/ml) in the experimental groups.

	Groups days			
	Control	Thiamine	CuONPs	CuONPs+ Thiamine
14	1.39±0.65 ^a	1.42±0.76	3.67±0.37 ^b	1.87±0.49 ^a
<i>P value</i>	<i>p>0.05</i>	<i>p>0.05</i>	<i>P<0.05</i>	<i>p>0.05</i>

a/b letters: Different letters indicate statistically significant differences between groups (P<0.05)

The SOD activity was not significantly differ neither between control and thiamine nor between CuO NPs and CuO NPs + Thiamine groups ($p>0.05$). However, it was significantly higher in the CuO NPs and CuO NPs + Thiamine groups than control and thiamine groups ($p<0.05$) (Table 5).

No significant difference was seen between control, thiamine and CuO NPs + Thiamine in the TAC ($P>0.05$). However, it was significantly lower in the CuO NPs group than other experimental groups ($P<0.05$) (Table 6).

No significant difference was seen between control, thiamine and CuO NPs + Thiamine in the MDA level ($P>0.05$). Administration of CuO NPs resulted in a significant increase in the level of MDA compared to the control, thiamine and CuO NPs + Thiamine groups ($P<0.05$). In contrast, the (CuO NPs + Thiamine) group exhibited a significantly lower MDA level compared to the CuO NPs group ($P<0.05$) (Table 7).

9. Discussion

In this study, exposure CuO NPs resulted in a significant decline in body weight and testicular mass.

Nanoparticles such as CuO NPs, owing to their extremely small size, can readily traverse cellular membranes including barriers such as the blood-testis barrier and accumulate in tissues, triggering oxidative stress and inflammatory responses that can lead to hepatotoxicity, neurotoxicity, and reproductive injury. Gastrointestinal absorption and accumulation of CuO NPs may also provoke digestive disturbances, impaired nutrient uptake, anorexia, negative energy balance, and consequential weight loss (1, 2).

In addition to the direct oxidative and inflammatory effects of CuO NPs on testicular tissue, the observed reduction in body weight likely contributed to the decreased testicular weight and spermatogenic damage. Systemic weight loss may reflect impaired nutrient absorption, lower energy availability, and reduced blood flow to peripheral organs, including the testes (1,3,4). These factors can exacerbate testicular atrophy and make germ cells more susceptible to oxidative stress, further compromising spermatogenesis. Therefore, the combined impact of systemic energy deficiency and direct nanoparticle-induced oxidative damage provides a more comprehensive explanation for the reductions in testis mass and germ cell

populations observed in the CuO NPs group.

The reproductive system is especially vulnerable to nanoparticulate toxicity. Germ cells undergo rapid mitotic and meiotic divisions and have elevated metabolic demands, which amplify their sensitivity to toxic insults. Moreover, the nanoscale transformation of CuO particles alters their physicochemical properties—such as increased surface area, solubility, and membrane permeability thereby facilitating intracellular uptake and intensifying cytotoxicity (3).

Accumulation of nanoparticles within testicular tissue can induce histological damage; apoptosis, necrosis, and degenerative changes, that disrupt the spermatogenic lineage and reduce populations of spermatogonia, spermatocytes, and spermatids. Because testis mass is largely a function of differentiated germ cells and seminiferous epithelium, suppression of spermatogenesis, impairment of Sertoli cell support, or reduction in seminiferous tubular fluid can all contribute to testicular weight loss. In addition, interference with androgen production or anti-androgenic effects of CuO NPs may further reduce the weight of accessory reproductive organs (4, 5).

CuO NPs may disrupt endocrine regulation by inhibiting pituitary gonadotropins (FSH and LH), thereby hindering testosterone synthesis, a hormone critical for spermatogenesis and maintenance of accessory sex organs. Elevated ROSs and protein oxidation can damage Leydig cells, while downregulation of steroidogenic acute regulatory protein (StAR) expression can limit cholesterol transport into mitochondria, further impairing steroidogenesis (6).

Oxidative stress is a predominant mechanism underlying CuO NP toxicity. These nanoparticles provoke a concentration-dependent increase in intracellular ROSs, which can oxidatively damage DNA, proteins, and lipids. Dissolution of CuO NPs releases free copper ions that participate in redox cycling, further amplifying ROSs production. This oxidative onslaught depletes cellular antioxidants e.g. glutathione, catalase, superoxide dismutase, elevates lipid peroxidation such as increased MDA, and ultimately precipitates cell injury and apoptosis (7, 8). Additionally, oxidative modifications such as protein carbonylation may disrupt normal cellular processes, and sustained activation of inflammatory pathways can exacerbate tissue damage (9).

Our results indicate that thiamine can ameliorate many of these deleterious effects. As an antioxidant, thiamine may enhance the activity of key enzymes e.g. catalase and SOD, scavenge free radicals, reduce lipid peroxidation, thus lowering MDA, and attenuate inflammatory responses, thereby helping to maintain cellular integrity in reproductive tissues (10, 11). Thiamine's role as a ligand in transport processes may facilitate its cellular uptake and antioxidant defense against ROSs and nanoparticle-induced stress (10).

Beyond its redox-modulating effects, thiamine might contribute to restoring hormonal balance disrupted by nanoparticle exposure. By decreasing oxidative stress, it may stabilize gene expression within steroidogenic pathways and support hormone synthesis, thus mitigating disturbances in the hypothalamic-pituitary-gonadal axis. Thiamine's antioxidant properties may also protect signaling pathways in Leydig, Sertoli, and germ cells from ROSs-induced dysregulation, preserving functions essential for spermatogenesis and endocrine homeostasis (12).

10. Conclusion

Exposure to CuO nanoparticles provoked significant histological and stereological damage in male reproductive tissues, including reduced seminiferous tubule diameter, lowered sperm density, disorganization of the reproductive epithelium, enlarged tubular lumens, interstitial edema, and depletion of spermatogenic cell populations, primarily attributable to oxidative stress and ROSs-mediated injury. Thiamine administration alleviated CuO NP-induced reproductive damage by preserving testicular structure and function through its antioxidant, anti-inflammatory, and endocrine-stabilizing effects, suggesting its potential as a therapeutic agent against nanoparticle-induced toxicity.

Acknowledgments

The authors wish to express their gratitude to Shahrekord University.

Conflict of Interest Disclosure

The authors declare that they have no conflicts of interest.

References

- [1] Devaraji M, Thanikachalam PV, Elumalai K. The potential of copper oxide nanoparticles in nanomedicine: A comprehensive review. *Biotechnol Notes*. 2024;5:80-99.
- [2] Harishchandra BD, Pappuswamy M, Antony P, Shama G, Pragatheesh A, Arumugam VA, et al. Copper nanoparticles: a review on synthesis, characterization and applications. *Asian Pacific journal of cancer biology*. 2020;5(4):201-10.
- [3] Naz S, Gul A, Zia M, Javed R. Synthesis, biomedical applications, and toxicity of CuO nanoparticles. *Appl Microbiol Biotechnol*. 2023;107(4):1039-61.

- [4] Salvo J, Sandoval C. Role of copper nanoparticles in wound healing for chronic wounds: literature review. *Burns Trauma*. 2022;10:tkab047.
- [5] Verma N, Kumar N. Synthesis and Biomedical Applications of Copper Oxide Nanoparticles: An Expanding Horizon. *ACS Biomater Sci Eng*. 2019;5(3):1170-88.
- [6] Yakut ZAC, Akcay GB, Çevik Ö, Şener G. Ameliorative effects of melatonin on intestinal oxidative damage in streptozotocin-induced diabetic rats. *Istanbul Journal of Pharmacy*. 2020;50(3):160-7.
- [7] Vassal M, Rebelo S, Pereira ML. Metal Oxide Nanoparticles: Evidence of Adverse Effects on the Male Reproductive System. *Int J Mol Sci*. 2021;22(15):8061.
- [8] Al-Musawi MMS, Al-Shmgani H, Al-Bairuty GA. Histopathological and Biochemical Comparative Study of Copper Oxide Nanoparticles and Copper Sulphate Toxicity in Male Albino Mice Reproductive System. *Int J Biomater*. 2022;2022(1):4877637.
- [9] Amiri A, Dehkordi RAF, Heidarnejad MS, Dehkordi MJ. Effect of the Zinc Oxide Nanoparticles and Thiamine for the Management of Diabetes in Alloxan-Induced Mice: a Stereological and Biochemical Study. *Biol Trace Elem Res*. 2018;181(2):258-64.
- [10] Luo Y, Zeng X, Dai X, Tian Y, Li J, Zhang Q, et al. Copper Oxide Nanoparticles Impair Mouse Preimplantation Embryonic Development through Disruption of Mitophagy-Mediated Metabolism. *ACS nano*. 2024;18(45):31244-60.
- [11] Kalirawana T, Sharma P, Joshi S. Reproductive toxicity of copper nanoparticles in male albino rats. *Int J Pharma Res Health Sci*. 2018;6(1):2258-63.
- [12] Dagar G, Bagchi G. Nanoparticles as potential endocrine disruptive chemicals. *NanoBioMedicine*. 2020:411-29.
- [13] Grigore ME, Biscu ER, Holban AM, Gestal MC, Grumezescu AM. Methods of Synthesis, Properties and Biomedical Applications of CuO Nanoparticles. *Pharmaceuticals (Basel)*. 2016;9(4):75.
- [14] Katsumiti A, Thorley AJ, Arostegui I, Reip P, Valsami-Jones E, Tetley TD, et al. Cytotoxicity and cellular mechanisms of toxicity of CuO NPs in mussel cells in vitro and comparative sensitivity with human cells. *Toxicol In Vitro*. 2018;48:146-58.
- [15] Fu X. Oxidative stress induced by CuO nanoparticles (CuO NPs) to human hepatocarcinoma (HepG2) cells. *Journal of Cancer Therapy*. 2015;6(10):889.
- [16] Moschini E, Colombo G, Chirico G, Capitani G, Dalle-Donne I, Mantecca P. Biological mechanism of cell oxidative stress and death during short-term exposure to nano CuO. *Sci Rep*. 2023;13(1):2326.
- [17] Chang Y-N, Zhang M, Xia L, Zhang J, Xing G. The toxic effects and mechanisms of CuO and ZnO nanoparticles. *Materials*. 2012;5(12):2850-71.
- [18] Naz S, Gul A, Zia M. Toxicity of copper oxide nanoparticles: a review study. *IET Nanobiotechnol*. 2020;14(1):1-13.
- [19] Abudayyak M, Guzel E, Ozhan G. Cupric Oxide Nanoparticles Induce Cellular Toxicity in Liver and Intestine Cell Lines. *Adv Pharm Bull*. 2020;10(2):213-20.
- [20] Samrot AV, Noel Richard Prakash LX. Nanoparticles Induced Oxidative Damage in Reproductive System and Role of Antioxidants on the Induced Toxicity. *Life (Basel)*. 2023;13(3):767.
- [21] Hu Y, Luo H, Netala VR, Li H, Zhang Z, Hou T. Comprehensive Review of Biological Functions and Therapeutic Potential of Perilla Seed Meal Proteins and Peptides. *Foods*. 2024;14(1):47.
- [22] Lukienko PI, Mel'nichenko NG, Zverinskii IV, Zabrodskaya SV. Antioxidant properties of thiamine. *Bull Exp Biol Med*. 2000;130(9):874-6.
- [23] Zimmermann M. Ethical guidelines for investigations of experimental pain in conscious animals. *Pain*. 1983;16(2):109-10.
- [24] Parasuraman S, Raveendran R, Kesavan R. Blood sample collection in small laboratory animals. *J Pharmacol Pharmacother*. 2010;1(2):87-93.
- [25] Fatahian Dehkordi RA, Bahadoran S, Alijani M, Mohebi A, Mohammadi H. Recovery effects of pomegranate seed powder on the testes following cadmium poisoning in Japanese quail (*Coturnix japonica*); a stereological and lipid peroxidation study. *Iranian Journal of Veterinary Science and Technology*. 2021;13(2):100-5.